



Test of long-range exchange-correlation kernels of time-dependent density functional theory at surfaces: Application to Si(111)2×1

O. Pulci,^{1,*} A. Marini,^{2,3,4} M. Palummo,² and R. Del Sole²

¹*ETSF, NAST, CNR-ISM, Dip.di Fisica, Università di Roma Tor Vergata, Via della Ricerca Scientifica 1, I-00133 Roma, Italy*

²*ETSF, NAST, Dip.di Fisica, Università di Roma Tor Vergata, Via della Ricerca Scientifica 1, I-00133 Roma, Italy*

³*IKERBASQUE, Basque Foundation for Science, E-48011 Bilbao, Spain*

⁴*Nano-Bio Spectroscopy Group, Dpto. Fisica de Materiales, Universidad del Pais Vasco, Bilbao, Spain*

(Received 16 August 2010; published 16 November 2010)

We present an application of time-dependent density-functional theory (TDDFT) to the study of the optical properties of the Si(111)2×1 surface from the infrared to the ultraviolet. We have carried out *ab initio* calculations using different methods, from DFT to Bethe-Salpeter equation (BSE) and, within TDDFT, we have tested the ability of different kernels to describe the optical features in a wide range of energies. We find good agreement between TDDFT and BSE results, by using in TDDFT a long-range frequency-dependent exchange-correlation kernel derived from the many-body formalism (the MB kernel). The agreement between theory and experiment is very good in the whole frequency range studied. Excitonic effects, important in the infrared part of the spectrum, are less pronounced in the visible and UV ranges.

DOI: [10.1103/PhysRevB.82.205319](https://doi.org/10.1103/PhysRevB.82.205319)

PACS number(s): 78.68.+m, 71.35.-y, 73.20.-r, 78.40.-q

I. INTRODUCTION

The inclusion of the electron-hole (e-h) interaction is crucial to obtain optical absorption spectra of nanostructures, surfaces, and bulk materials in good agreement with experiments.^{1,2} Such interaction leads to two effects: the creation of bound electron-hole states (excitons) within the one-particle gap, and a distortion of the continuous spectrum above the gap. Both effects are generally present, though bound excitons are not observed when the e-h interaction is so weak that their binding energy is smaller than the thermal broadening or the experimental resolution. The first *ab initio* calculation of optical spectra with the inclusion of excitonic effects by solving the Bethe-Salpeter equation (BSE) within many-body perturbation theory (MBPT) appeared in 1995 (Ref. 3) for a small molecular cluster. Only in 1998, however, the case of excitons in extended systems was studied.⁴⁻⁶ The ingredients of the calculations have a simple physical meaning (the bare and screened e-h interactions, v and W , respectively) and the results compare well with experimental data.

The BSE is generally rewritten as an eigenvalue problem whose dimension is given by the number of e-h pairs considered. As a consequence, its solution can be particularly demanding, preventing its application to complex systems like surfaces. In fact, in these systems the large number of single-particle states dramatically increases the dimension of the BS equation.

An alternative approach to calculate the absorption spectra is the time-dependent density-functional theory (TDDFT).⁷ In the last years TDDFT has emerged as a powerful tool for the description of excited states (especially for finite and molecular systems)^{8,9} alternative to more cumbersome quantum chemical methods such as configuration interaction. TDDFT is, in principle, exact for neutral excited-state properties, and its simplicity relies on the fact that the two-point response function $\chi(r, r', \omega)$ is needed, instead of the four-point function of the Bethe-Salpeter approach.

However, the exact exchange-correlation (xc) kernel (f_{xc}), a key ingredient of TDDFT, is unknown; hence approximations are employed. The simplest and most commonly used, the adiabatic local-density approximation (ALDA or TDLDA), is known to fail in extended systems (such as surfaces). More refined kernels have been recently proposed¹⁰⁻¹³ but never tested on surfaces. In,^{10,14} a nonlocal, static kernel with the correct long-range behavior has been successfully applied to three-dimensional systems. In Refs. 11-13 a more elaborated nonlocal and energy-dependent f_{xc} , derived within the MB framework, has been presented; it has been applied, up to now, only to one-dimensional¹⁵ and three-dimensional¹¹⁻¹³ systems, yielding spectra very similar to BSE and experimental ones.

In this paper, we study the performance of the MB TD-DFT kernel, proposed in Refs. 11-13, to calculate the optical spectra of the Si(111)2×1 surface: a paradigmatic two-dimensional system. This surface exhibits clear bound surface-state excitons that have been already described theoretically¹⁶ by using the Bethe-Salpeter equation. In particular, we show here that this MB-based kernel reproduces the bound excitons in the infrared (IR) energy range of the Si(111)2×1 surface, and also correctly describes the high-energy range. We calculate the linear response of the surface up to the visible and ultraviolet energy range (where only tight-binding calculations¹⁷ have been carried out so far), explaining the differences with respect to the independent particle approximation in terms of correlation effects. Moreover, we test the reliability of a simpler long-range, nonlocal, and energy-independent kernel,¹⁰ to describe both regimes.

II. TIME-DEPENDENT DENSITY-FUNCTIONAL THEORY

TDDFT is, in principle, exact and represents a promising and simple alternative to the BSE. Indeed, TDDFT requires the knowledge of the density response function $\chi(r, t; r', t')$,

in contrast to the BS equation where the full, four-point, e-h Green's function is needed.

TDDFT casts all many-body effects into the dynamical exchange-correlation kernel $f_{xc}(\vec{r}, t; \vec{r}', t') = \delta v_{xc}(\vec{r}, t) / \delta \rho(\vec{r}', t')$, where $v_{xc}(\vec{r}, t)$ is the time-dependent exchange-correlation potential. The absorption spectra can be rewritten in terms of the time Fourier transformed χ , that TDDFT defines as a solution of a Dyson-type equation

$$\chi(\vec{r}, \vec{r}'; \omega) = \chi_0(\vec{r}, \vec{r}'; \omega) + \int \int d\vec{r} d\vec{r}'' \chi_0(\vec{r}, \vec{r}''; \omega) \times \left[\frac{1}{|\vec{r}'' - \vec{r}'|} + f_{xc}(\vec{r}'', \vec{r}''; \omega) \right] \chi(\vec{r}'', \vec{r}'; \omega), \quad (1)$$

with $\chi_0(\vec{r}, \vec{r}'; \omega)$ the independent-particle susceptibility. A reliable calculation of the absorption spectra depends on how good is the approximation used to describe $f_{xc}(\vec{r}, \vec{r}'; \omega)$.

The simplest approximation, the adiabatic extension of the static LDA (ALDA), is surprisingly good in molecules and small clusters,⁸ where the Hartree contribution is dominant. However, in extended systems, where the xc component (f_{xc}) becomes more important, ALDA fails in describing excitonic effects.¹⁸ This failure has been traced back to the lack, in the ALDA, of the long-range spatial tail of the kernel, reflecting the $-1/r$ electron-hole interaction at large distances.¹² In the last years several attempts to include the correct long-range tails have been proposed. A simplified scheme, proposed in 2002 by Reining *et al.*,¹⁰ consists in approximating the TDDFT kernel, in momentum space, with the expression $-\alpha/q^2$, which, by construction, has the right asymptotic behavior of the exact TDDFT kernel. Here, we refer to this kernel as the Reining Onida Rubio Olevano (RORO). The constant α is material dependent and can be determined by fitting the bulk optical spectra.^{14,19}

Instead, starting from the many-body framework, several groups, following different approaches, have shown in the last years that it is possible to derive a spatially nonlocal and energy-dependent kernel that is completely parameter free. Reining and co-workers¹¹ have assumed the equivalence of the four-point polarizability of the BS equation with the two-point polarizability of TDDFT, that is rigorous only for the two-point contraction of the BS equation polarizability. An alternative approach,^{12,13} instead, used the BS equation to derive a perturbative expansion of the f_{xc} in powers of the screened e-h interaction W . The first order of this expansion, shown in Eq. (2), reduces to the expression found by Reining and co-workers. This same first-order expression for f_{xc} has been later obtained by using a density-functional approach to the MBPT.²⁰ From now on, we will refer to this kernel as to the MB kernel.

The MB xc-kernel f_{xc}^{MB} has been shown to yield optical spectra of bulk semiconductors^{11,12} and insulators¹³ in very good agreement with BS equation results and experiment. Noticeably, f_{xc}^{MB} has been proved to correctly account for strongly bound excitons in wide-gap insulators, such as LiF and SiO₂,¹³ and in one-dimensional polymers.¹⁵

According to Refs. 12 and 13, the MB xc kernel is written as

$$f_{xc}^{MB}(\vec{r}, \vec{r}'; \omega) = \int \int d\vec{r} d\vec{r}'' \chi_{QP}^{-1}(\vec{r}, \vec{r}''; \omega) P^{(1)}(\vec{r}, \vec{r}''; \omega) \chi_{QP}^{-1}(\vec{r}'', \vec{r}'; \omega), \quad (2)$$

$P^{(1)}$ being the first order W contribution to the irreducible polarizability P .²¹ $P^{(1)}$ is strictly related to the exciton Hamiltonian, which, however, is not diagonalized in this approach. The perturbative stability of f_{xc} is ensured by the exact inclusion of the GW induced gap correction in the quasiparticle polarizability χ_{QP} to all orders.¹³ Then, the irreducible polarizability is calculated according to the TD-DFT formulation,

$$P(\omega) = \chi_{QP}(\omega) + \chi_{QP}(\omega) f_{xc}^{MB}(\omega) P(\omega). \quad (3)$$

Since P and f_{xc} are all two-point quantities, TDDFT is, in principle, computationally less demanding than the BS equation and could be employed in the case of more complex systems, such as surfaces, nanostructures, biological molecules, etc., where the BS equation is hardly usable. Surfaces are particularly difficult to study, since a large number of k points and of transitions must be included in the excitonic Hamiltonian. As a consequence, the optical spectra of surfaces are, in general, calculated in a small energy range above the gap, in order to reduce as much as possible the dimension of the BS kernel. Although TDDFT provides a potentially efficient tool to overcome this limitation, the performance of the MB xc-kernel is unknown in the two-dimensional case. Testing the performance of this kernel is the main purpose of this work.

III. Si(111)2×1 SURFACE

The Si(111)2×1 surface reconstruction is well described by Pandey's π -bonded chain model,²² where the atoms in the first layer form zigzag chains along the $[1\bar{1}0]$ direction. Filled and empty surface bands occur within (or close to) the bulk gap, due to the dangling bonds of first-layer atoms. The first determination of surface states with optical means appeared in 1968 when Chiarotti and co-workers measured the surface differential reflectivity (SDR) of Ge(111)2×1.²³ In SDR experiments, the reflectance of the chemisorbed surface (oxidized in that case) is subtracted from that of the clean surface, the difference being surely related to the surface. In 1971 a similar experiment was carried out on Si(111)2×1. SDR shows, for both materials, a peak at 0.45 eV, related to transitions across surface states.²⁴ Later SDR experiments, carried out with polarized light, showed that these peaks occur just for light polarized along the surface chains²⁵ (y polarization in Fig. 1). Such large anisotropy in surface optical properties is a clear-cut demonstration of the validity of Pandey's chain model for Si and Ge(111)2×1 surfaces.

Optical spectra have been measured for Si(111)2×1 not only in the infrared,^{24,25} where transitions across surface states occur, but also in the visible and ultraviolet, up to 3.5 eV, by SDR (see Fig. 1) (Ref. 26) and up to 4.5 eV by reflectance anisotropy spectroscopy (RAS) (Refs. 27 and 28) (see Fig. 2). RAS (Ref. 29) is an experimental technique used nowadays as a practical tool to characterize surfaces

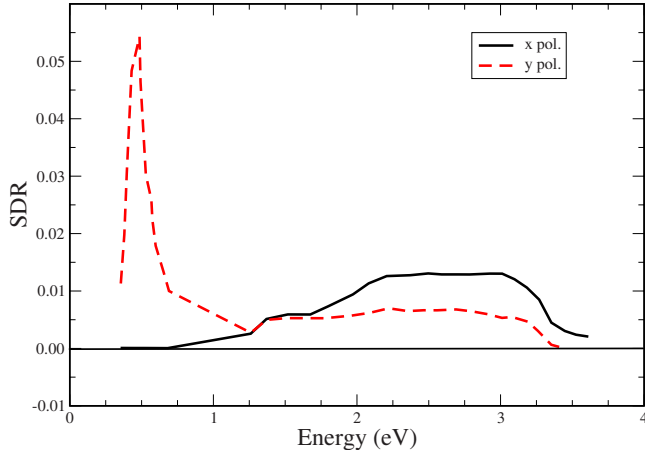


FIG. 1. (Color online) Experimental SDR spectrum of Si(111) 2×1 for light polarized along the silicon surface chains (y polarization, red dashed line) and perpendicular to the chains (x polarization, black line) (Ref. 26); y is the $[1\bar{1}0]$ direction, x is the $[1\bar{1}\bar{2}]$.

and interfaces. It is a high resolution and nondestructive optical technique that achieves surface sensitivity by measuring the difference in reflectivity of normal incident light, for two perpendicular directions on a surface. This geometry leads to a cancellation of the bulk isotropic contribution for cubic crystals.

The reflectance anisotropy spectrum is defined as

$$\frac{\Delta R}{R} = \frac{\Delta R_y - \Delta R_x}{R},$$

where $\frac{\Delta R_i}{R}$ is the correction (for light polarized along the i direction) to Fresnel's reflectivity, accounting for the nonlocality, anisotropy, and inhomogeneity of the surface dielectric tensor. In a repeated slab geometry the RA signal turns out to be equal to

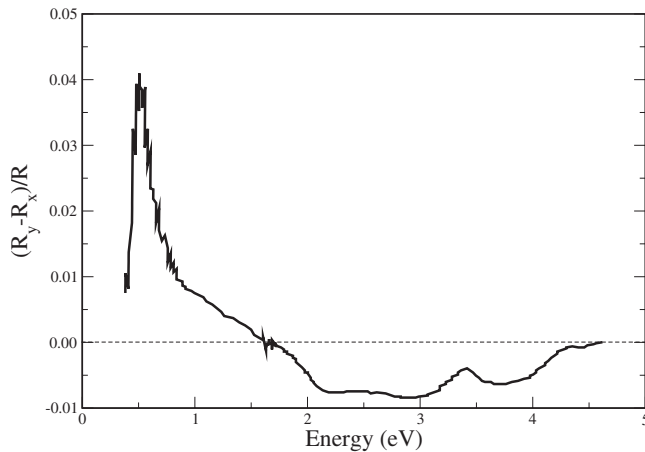


FIG. 2. Experimental RAS spectrum of Si(111) 2×1 by Goletti *et al.* (Ref. 28), y is the $[1\bar{1}0]$ direction (parallel to the chains), x is the $[1\bar{1}\bar{2}]$ (perpendicular to the chains).

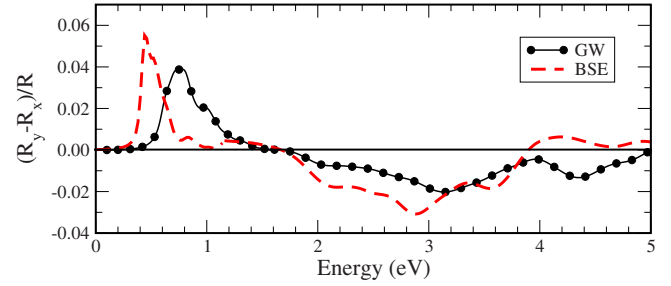


FIG. 3. (Color online) Calculated RAS for Si(111) 2×1 within GW and BSE. y is the $[1\bar{1}0]$ direction (parallel to the chains), x is the $[1\bar{1}\bar{2}]$ (perpendicular to the chains).

$$\frac{\Delta R_i}{R} = \frac{4\omega d}{c} \text{Im} \frac{4\pi\alpha_{ii}^{hs}}{\epsilon_{bulk} - 1},$$

where α_{ii}^{hs} is the half-slab polarizability.³⁰ This can be calculated according to various approximations, even including MB effects within BSE or TDDFT.

Tight-binding calculations³¹ first, and BS equation calculations later,¹⁶ have shown that the optical spectrum of this surface in the infrared range is dominated by a quasi-one-dimensional surface-state exciton, with large binding energy (0.27 eV), that takes most of the oscillator strength of the transitions across surface states. According to this picture, this bound exciton generates the absorption peak appearing in experiments at 0.45 eV (Refs. 24, 27, and 28) (see Figs. 1 and 2), whose observed asymmetry is most probably due to phonon replicas. The peak calculated within the independent quasiparticle approximation (GW) occurs instead at about 0.8 eV (see Fig. 3). For what concerns the visible range, RAS calculations have been carried out so far only within a single-particle, semiempirical tight-binding scheme.¹⁷

Here, we will first show BS equation calculations from the infrared to the UV, then we will use them as a benchmark to assess the accuracy of the TDDFT approach.

IV. QUASIPARTICLE CORRECTIONS

In agreement with previous results,^{16,32} a GW minimum gap of about 0.75 eV between the surface states (near \bar{J}) is obtained.³³ While the quasiparticle electronic gap between surface states opens, with respect to the DFT-LDA states, by about 0.4–0.5 eV, the GW corrections between bulk states are about 0.6–0.7 eV. The resulting quasiparticle surface band gaps are shown in Table I, where also experimental data taken from Refs. 34–37 are reported. As in previous works,^{16,32} the agreement with experiments is good, also considering the significant discrepancy between the data, which are obtained using different techniques. This point has been discussed in details in Ref. 31, and in the case of highly n -doped samples will be the object of a forthcoming publication.³⁸

V. OPTICAL SPECTRA

The RAS spectrum calculated within the independent-quasiparticle approximation (GW) is shown in Fig. 3. The

TABLE I. Electronic gaps at the surface high-symmetry points. Values are in electron volt.

	\bar{J}	\bar{K}	\bar{J}'
DFT	0.34	0.61	1.67
GW	0.8	1.0	2.4
Expt.	0.6, ^a 0.75, ^b 0.5 ^c		

^aReference 34.

^bReference 35 and 36.

^cReference 37.

infrared peak appears at ~ 0.8 eV, while it occurs at 0.45 eV in the experiments. Using the BSE (Ref. 39) (see Fig. 3), we recover the results of the calculations of Reining and Del Sole (carried out in 1991 within semiempirical tight binding)³¹ and of the more recent *ab initio* BSE calculations by Rohlfing and Louie.¹⁶ The BSE predicts a strongly bound exciton at about 0.45 eV in both cases.

GW calculations show a qualitative agreement with the experiment (see Fig. 2). We distinguish three different energy regimes, as related to the character of the optical transitions: in the IR ($E < 1.1$ eV) the RAS is dominated by a sharp surface exciton peak. Below the bulk direct gap ($E < 3.4$ eV) we observe mixed surface-state/bulk-state excitations, that turn to purely bulk-state transitions above it ($E > 3.4$ eV). The BSE results are overall similar to GW ones but improve the agreement with the experimental RAS shown in Fig. 2. The agreement between theory and experiment is surprisingly good also for the fine details in the visible: the experimental RAS has negative structures at 2.1 and 3 eV and a negative plateau in between, a spike at 3.4 eV, and a valley centered at 3.8 eV. Similar structures appear in the BSE spectrum at about the same energies. However, a discrepancy occurs as far as the intensity is concerned: the calculated RAS in the visible and UV overestimates the experiment by a factor 3. This is a general feature of RAS spectra,^{40–42} probably due to the presence of multiple domains, steps, surface imperfections, etc. A detailed discussion of this point for Si(100) is given in Ref. 41.

The key point is now to see whether it is possible to properly include electronic correlations in the optical spectra by means of TDDFT. A simple test clearly shows the inability of TDLDA to improve the calculated spectrum with respect to a standard DFT-LDA calculation (Fig. 4) in the IR region. The TDLDA spectrum is very similar to the LDA spectrum, and important discrepancies remain with respect to experiment.

In contrast, by using the f_{xc}^{MB} we find a very good agreement with the BSE and experiment. The surface contributions to reflectance for x and y polarization, perpendicular and parallel to the chains, are compared in Fig. 5 with those obtained by solving the BS equation. It is clear that the agreement between BS equation and TDDFT in the present formulation is very good: with a MB-derived long-range kernel TDDFT is able to reproduce BS equation results, even where surface state transitions give rise to bound excitons.

The high-energy structures in Fig. 5 can be interpreted as the contribution of the E_1 bulk resonant exciton occurring

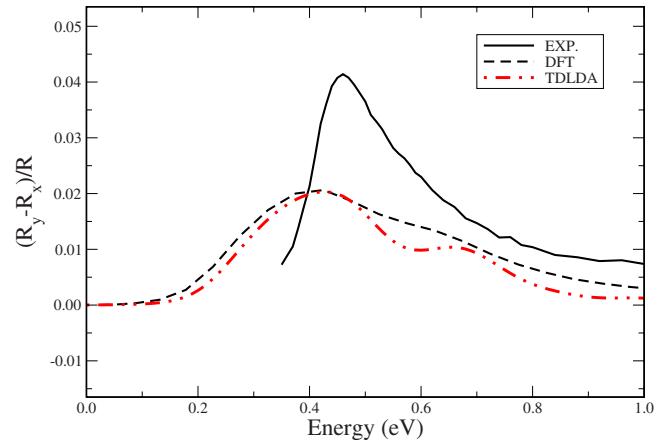


FIG. 4. (Color online) RAS calculated within DFT-LDA and TDLDA, compared with experiment (Ref. 25). A broadening of 0.05 eV has been used in the calculated spectra.

close to 3.4 eV, with a low-frequency spread due to surface-allowed indirect transitions; the valley at 4.5 eV is due to surface perturbation on the E_2 peak.

The RAS, calculated within the BS equation and TDDFT approaches, is shown in Fig. 6. Again, the agreement is very good for the excitonic peak in the infrared, and good in the visible. The main discrepancy between the two curves is just around 3.4 eV, and can be explained by the fact that the RAS arises from small differences between the spectra calculated for different polarizations of light. As a result, the small differences between BS equation and TDDFT for the two polarizations shown in Fig. 5, after subtraction, can yield, at some frequencies, a bigger difference in the RAS, as evident in Fig. 6. Nevertheless, we can conclude that BSE and TDDFT give results in fairly good agreement also for the RAS.

A crucial aspect of the present TDDFT method is that it is computationally more advantageous than the BS equation. The BS exciton Hamiltonian for the present Si(111)2 \times 1 surface is as large as 100 000 \times 100 000. In contrast the Fourier transform of Eq. (1) reduces to the inversion, at each

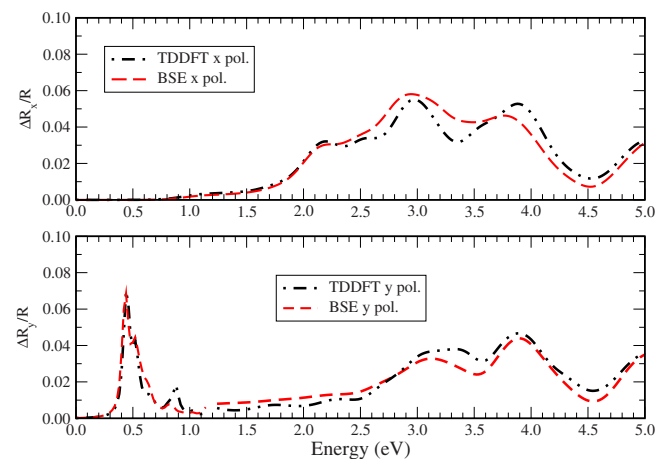


FIG. 5. (Color online) Calculated surface contribution to reflectance for light polarized along x (perpendicular to the chains) and along y (parallel to the chains) within TDDFT (many-body kernel) and BSE.

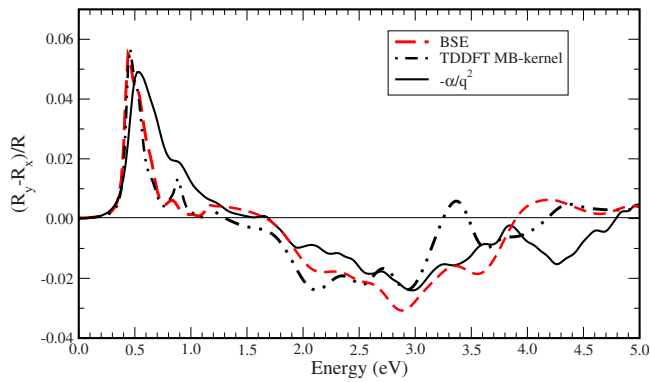


FIG. 6. (Color online) Calculated RAS for Si(111) 2×1 within TDDFT (many-body kernel), TDDFT-RORO kernel ($\alpha=+0.2$), and BS equation.

frequency, of a 100×100 matrix, three orders of magnitude smaller than the BS hamiltonian. Moreover to calculate $P^{(1)}$ [see Eq. (2)], the BS Hamiltonian must not be diagonalized.

An even simpler approach to calculate optical spectra is based on the use the nonlocal, but energy-independent kernel, known as the RORO kernel: $f_{xc} = -\alpha/q^2$.¹⁰ Here we check its ability to describe the RAS of the Si(111) surface at high and low energies, namely, in the regions of weak excitonic effects and of bound excitons, respectively. We have performed the test for $\alpha=0.2$, which is appropriate for bulk Si (in this way, we do not introduce additional parameter for the surface). The results are shown in Fig. 6. The agreement with the BS equation results is fairly good in both regimes. The main discrepancy is that the exciton binding energy is slightly underestimated within the RORO approach. This is probably due to the fact that surface screening of the e-h interaction is weaker than bulk screening described by the bulk α value. On the other hand, it is already known that the RORO kernel does not give an accurate description of excitonic effects when they are strong, as in insulators.⁴³ In conclusion, we argue that the RORO kernel can be applied, without additional parameters, to surfaces of semiconductors with not too strong excitonic effects. In these cases, the reduced accuracy of the RORO method is more than compensated by the dramatic reduction in the computational work: the kernel is calculated at once in terms of the parameter α ,

without calculating nor diagonalizing the exciton Hamiltonian. The computational complexity is the same as that of a single-particle calculation.

VI. CONCLUSIONS

We have carried out wide range calculations of the optical properties of the prototypical surface Si(111) 2×1 , from the infrared to the UV range. We confirm that a strongly bound surface-state exciton appears in the infrared, close to the experimental value of 0.45 eV, while only weak excitonic effects occur at higher frequencies. The inclusion of excitonic effects is however crucial to obtain a quantitative agreement with experiment in the high-energy region.

Moreover, we have carried out TDDFT calculations for the optical properties of a surface using the many-body kernel. The agreement with BS equation results is very good, both for transitions across surface states, where strong excitonic effects occur, and for bulklike transitions. This is a demonstration that TDDFT is able to reproduce BSE results also at surfaces. Together with the early demonstrations that this kernel works well in three dimensions, and more recent demonstrations that it works well in 0 and 1 dimension, we have finally shown that the approach of Eqs. (1) and (2) may yield good optical spectra, in very good agreement with those coming from the solution of the BS equation, in all systems, from zero to three dimensions.

Finally, we have also carried out optical spectra calculations for Si(111) 2×1 using the static $-\alpha/q^2$ kernel proposed in Ref. 10. In this case the agreement with BS results slightly worsens but it is still satisfactory. If such kind of agreement will be confirmed by calculations for other surfaces, the RORO method could become a simple and computationally unexpensive approach to the optical properties of surfaces with weak excitonic effects.

ACKNOWLEDGMENTS

CPU time granted by CINECA, ENEA CRESCO, and CASPUR is gratefully acknowledged. The research leading to these results has received funding from the European Community's Seventh Framework Programme (FP7/2007-2013) under grant Agreement No. 211956.

*Author to whom correspondence should be addressed; olivia.pulci@roma2.infn.it

¹G. Onida, L. Reining, and A. Rubio, *Rev. Mod. Phys.* **74**, 601 (2002), and references therein.

²M. Rohlfing and S. G. Louie, *Phys. Rev. B* **62**, 4927 (2000), and references therein.

³G. Onida, L. Reining, R. W. Godby, R. Del Sole, and W. Andreoni, *Phys. Rev. Lett.* **75**, 818 (1995).

⁴S. Albrecht, L. Reining, R. Del Sole, and G. Onida, *Phys. Rev. Lett.* **80**, 4510 (1998).

⁵L. X. Benedict, E. L. Shirley, and R. B. Bohn, *Phys. Rev. Lett.* **80**, 4514 (1998).

⁶M. Rohlfing and S. G. Louie, *Phys. Rev. Lett.* **80**, 3320 (1998).

⁷E. Runge and E. K. U. Gross, *Phys. Rev. Lett.* **52**, 997 (1984).

⁸I. Vasiliev, S. Oğüt, and J. R. Chelikowsky, *Phys. Rev. Lett.* **86**, 1813 (2001).

⁹B. Walker, A. M. Saitta, R. Gebauer, and S. Baroni, *Phys. Rev. Lett.* **96**, 113001 (2006).

¹⁰L. Reining, V. Olevano, A. Rubio, and G. Onida, *Phys. Rev. Lett.* **88**, 066404 (2002).

¹¹F. Sottile, V. Olevano, and L. Reining, *Phys. Rev. Lett.* **91**, 056402 (2003).

¹²G. Adragna, R. Del Sole, and A. Marini, *Phys. Rev. B* **68**, 165108 (2003).

- ¹³A. Marini, R. Del Sole, and A. Rubio, *Phys. Rev. Lett.* **91**, 256402 (2003).
- ¹⁴P. Gori, M. Rakel, C. Cobet, W. Richter, N. Esser, A. Hoffmann, R. Del Sole, A. Cricenti, and O. Pulci, *Phys. Rev. B* **81**, 125207 (2010).
- ¹⁵D. Varsano, A. Marini, and A. Rubio, *Phys. Rev. Lett.* **101**, 133002 (2008).
- ¹⁶M. Rohlffing and S. G. Louie, *Phys. Rev. Lett.* **83**, 856 (1999).
- ¹⁷A. Selloni, P. Marsella, and R. Del Sole, *Phys. Rev. B* **33**, 8885 (1986).
- ¹⁸V. Olevano, M. Palummo, G. Onida, and R. Del Sole, *Phys. Rev. B* **60**, 14224 (1999).
- ¹⁹S. Botti, F. Sottile, N. Vast, V. Olevano, L. Reining, H. C. Weisker, A. Rubio, G. Onida, R. Del Sole, and R. W. Godby, *Phys. Rev. B* **69**, 155112 (2004).
- ²⁰F. Bruneval, F. Sottile, V. Olevano, R. DelSole, and L. Reining, *Phys. Rev. Lett.* **94**, 186402 (2005).
- ²¹The approach proposed by Sottile (Ref. 11), uses as zero-order response function the KS one and includes in Eq. (2) an additional contribution: f_{xc}^{QP} . This term is first order in the self-energy, and it should account for the QP corrections to the Kohn-Sham energy levels. In Ref. 13 it is argued that this contribution is not stable, hence self-energy corrections are usually embodied in the zeroth-order GW response function.
- ²²K. C. Pandey, *Phys. Rev. Lett.* **49**, 223 (1982).
- ²³G. Chiarotti, G. Del Signore, and S. Nannarone, *Phys. Rev. Lett.* **21**, 1170 (1968).
- ²⁴G. Chiarotti, S. Nannarone, R. Pastore, and P. Chiaradia, *Phys. Rev. B* **4**, 3398 (1971).
- ²⁵P. Chiaradia, A. Cricenti, S. Selci, and G. Chiarotti, *Phys. Rev. Lett.* **52**, 1145 (1984).
- ²⁶S. Selci, P. Chiaradia, F. Ciccacci, A. Cricenti, N. Sparvieri, and G. Chiarotti, *Phys. Rev. B* **31**, 4096 (1985).
- ²⁷C. Goletti, G. Bussetti, F. Arciprete, P. Chiaradia, and G. Chiarotti, *Phys. Rev. B* **66**, 153307 (2002).
- ²⁸C. Goletti, G. Bussetti, P. Chiaradia, and G. Chiarotti, *J. Phys.: Condens. Matter* **16**, S4289 (2004).
- ²⁹D. E. Aspnes, J. F. Harbison, A. A. Studna, and L. T. Florez, *J. Vac. Sci. Technol. A* **6**, 1327 (1988); P. Weightman, D. S. Martin, R. J. Cole, and T. Farrell, *Rep. Prog. Phys.* **68**, 1251 (2005).
- ³⁰F. Manghi, E. Molinari, R. Del Sole, and A. Selloni, *Phys. Rev. B* **39**, 13005 (1989).
- ³¹L. Reining and R. Del Sole, *Phys. Rev. Lett.* **67**, 3816 (1991).
- ³²J. E. Northrup, M. S. Hybertsen, and S. G. Louie, *Phys. Rev. Lett.* **66**, 500 (1991).
- ³³We have carried out a DFT-LDA calculation to optimize the geometry, by using a 12 layers slab plus six layers of vacuum, and 20 Ry cutoff in the kinetic energy. Test calculations performed at 30 Ry have shown negligible differences. The ground-state calculations have been carried on by using ABINIT and FHI98MD (Refs. 44 and 45). Both codes have yielded a buckling of 0.53 Å for the first-layer silicon atomic chains. As a second step, we performed a quasiparticle calculation correcting the DFT eigenvalues within the perturbative GW scheme (Refs. 46 and 47).
- ³⁴R. M. Feenstra, W. A. Thompson, and A. P. Fein, *Phys. Rev. Lett.* **56**, 608 (1986); J. A. Stroschio, R. M. Feenstra, and A. P. Fein, *ibid.* **57**, 2579 (1986).
- ³⁵R. I. G. Uhrberg, G. V. Hansson, J. M. Nicholls, and S. A. Flodström, *Phys. Rev. Lett.* **48**, 1032 (1982).
- ³⁶P. Perfetti, J. M. Nicholls, and B. Reihl, *Phys. Rev. B* **36**, 6160 (1987).
- ³⁷P. Martensson, A. Cricenti, and G. V. Hansson, *Phys. Rev. B* **32**, 6959 (1985).
- ³⁸G. Bussetti *et al.* (unpublished).
- ³⁹We have calculated the optical spectra by using the YAMBO package (Ref. 48) by solving the BS and the TDDFT equations. We used 128 k points in the BZ, 3999 plane waves. The screening has been calculated using 45 q points in the IBZ and 503 G vectors. TDLDA and TDDFT calculations with the RORO kernel have been performed using the code DP, <http://www.dp-code.org>, 48 filled states and 40 empty states have been included. 531 plane waves (107 in the exchange term) have been used.
- ⁴⁰J. R. Power, O. Pulci, A. I. Shkrebtii, S. Galata, A. Astroppekakis, K. Hinrichs, N. Esser, R. Del Sole, and W. Richter, *Phys. Rev. B* **67**, 115315 (2003).
- ⁴¹M. Palummo, N. Witkowski, O. Pluchery, R. Del Sole, and Y. Borenstein, *Phys. Rev. B* **79**, 035327 (2009).
- ⁴²M. Marsili, N. Witkowski, O. Pulci, O. Pluchery, P. L. Silvestrelli, R. D. Sole, and Y. Borenstein, *Phys. Rev. B* **77**, 125337 (2008).
- ⁴³V. Garbuio, M. Cascella, L. Reining, R. Del Sole, and O. Pulci, *Phys. Rev. Lett.* **97**, 137402 (2006); R. Del Sole, O. Pulci, V. Olevano, and A. Marini, *Phys. Status Solidi B* **242**, 2729 (2005).
- ⁴⁴First-principles computation of material properties: the ABINIT software project, <http://www.abinit.org>, X. Gonze, J.-M. Beuken, R. Caracas, F. Detraux, M. Fuchs, G.-M. Rignanesse, L. Sindic, M. Verstraete, G. Zerah, F. Jollet, M. Torrent, A. Roy, M. Mikami, Ph. Ghosez, J.-Y. Raty, and D. C. Allan, *Comput. Mater. Sci.* **25**, 478 (2002).
- ⁴⁵M. Bockstedte, A. Kley, J. Neugebauer, and M. Scheffler, *Comput. Phys. Commun.* **107**, 187 (1997).
- ⁴⁶L. Hedin, *Phys. Rev.* **139**, A796 (1965).
- ⁴⁷M. S. Hybertsen and S. G. Louie, *Phys. Rev. B* **35**, 5585 (1987); R. W. Godby, M. Schlüter, and L. J. Sham, *ibid.* **37**, 10159 (1988).
- ⁴⁸A. Marini, C. Hogan, M. Grüning, and D. Varsano, *Comput. Phys. Commun.* **180**, 1392 (2009).